

Design of Space Environment module for Validation of Attitude Control Algorithms for LEO Satellites

Umar Mufti¹, Atiq-ur-Rehman²

AOCS Section, Satellite Research & Development Centre-Karachi,(SUPARCO) Pakistan

Email: umar_nedian@yahoo.com , atiq2k@gmail.com

Abstract: This paper describes the design of space environment module that is used for validation of Attitude Determination and Control Systems (ADCS) control algorithms for LEO Satellites. This module is the major block of a complete AOCS simulator, the other blocks of which are the sensors, actuators and control algorithms. The space environment module includes orbit propagator, GPS time, Sun model, magnetic field model and spacecraft attitude kinematics and dynamics. The performance of the module will be evaluated using Komsat-1 spacecraft. The Komsat-1 results are generated in Satellite Tool Kit (STK) which will serve as a reference for space environment results verification.

Keywords: LEO Satellites, space environment, spacecraft attitude kinematics, spacecraft dynamics, orbit propagator, GPS time, Sun model, magnetic field model

1 INTRODUCTION

The needs for the modeling and computer simulations are increasing with the rapid increase in the demands of space industry. It is not possible to perform all the real tests at the start of a space project. The AOCS simulator provides the toolbox to simulate the satellite in space based on the mission requirements and to finalize the attitude and orbit control algorithms. The real tests of these algorithms are then performed and fine tuning of the controlling gains are done.

The space environment module is an essential part of the AOCS simulator that simulates the spacecraft in space and provides the space environment at which the control algorithms will work on. The tool acts as a preliminary module before the real hardware implementation of the AOCS design. The module will be generalized and configurable and can be used for low earth orbits whenever the new mission requirements are furnished.

2 REFERENCE FRAMES

To analyze the motion of a satellite, it is necessary to define reference frames with which the satellite motion will be referenced. The four reference frames used in the space environment module are the

1. Earth-Centered Inertial (ECI) Reference Frame,
2. Earth-Centered Fixed (ECF) Reference Frame,
3. Body Coordinate System, and the
4. Perifocal Coordinate System

The **Z**-axis of the ECI is the rotation axis of the Earth, towards the celestial north pole, and the **X-Y** plane is the equatorial

plane of the Earth. The vernal equinox vector is selected to be the **X**-axis and finally the direction of the **Y**-axis completes a right handed orthogonal frame represented in Figure 1. The second reference frame has its origin located at the center of the Earth. The **X** and **Y** axes rotate with the Earth relative to the ECI frame about the **Z**-axis as shown in Figure 2. It has a rotation rate of $\omega_e = 7.2921 \times 10^{-5}$ rad/s. The **X**-axis points toward the intersection between the Greenwich meridian and the Equator, which represents zero degree longitude and zero degree latitude, and the **Y** axis completes the right handed orthogonal system.

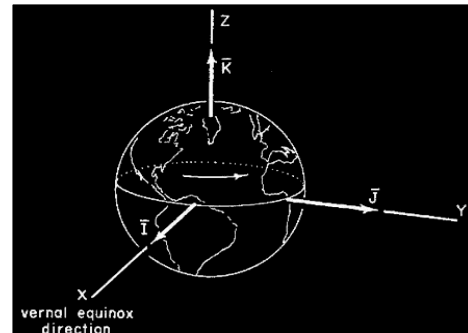


Figure 1 - Earth-Centred Inertial (ECI) Frame

The third coordinate system has its origin located in the satellite center of mass and rotates with the satellite at angular rate, and the axes are locked to the satellite and coincide with the satellite principal axes of inertia. The fourth coordinate system, see Figure 3, is used for describing the motion of the satellite. The fundamental plane is the satellite's orbit. The **X**-axis points towards the perigee and **Y**-axis is orthogonal to **X**-axis in the orbital plane. The **Z**-axis is directed along the angular momentum, **h** of the satellite orbit. One other reference frame, that is, the Orbit Coordinate Frame is used, when the complete Attitude and Orbit Control System (AOCS) Simulator for all the AOCS mission modes is to be designed, which is beyond the scope of this paper.

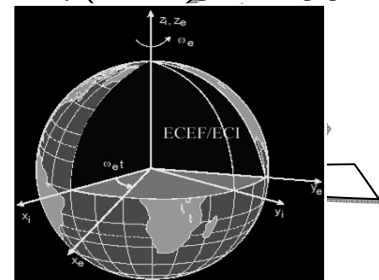


Figure 2 - Earth-Centered Fixed (ECF) Frame, subscript 'i' for ECI and 'e' for ECF reference frames respectively

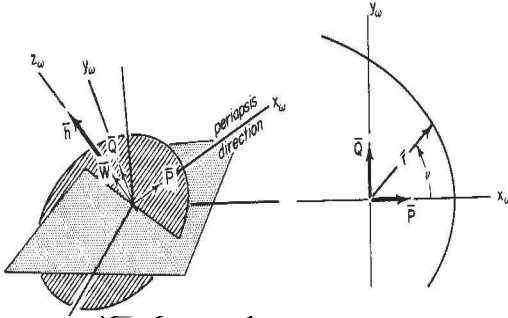


Figure 3 - Perifocal Coordinate Frame

3 EPOCH CLOCK

The simulation time and date are generated from this block. The initial parameters for the date are set in Gregorian UTC time. The block generates the Julian date (JD) and JD2000. The Julian date is converted to JD2000 using

$$jd = 367 (yr) - floor \left[\frac{7}{4} (yr + floor \left(\frac{mo + 9}{12} \right)) \right] + floor \left[\frac{275}{9} (mo) \right] + d + 1721013.5 + \frac{1}{24} \left(\frac{1}{60} (60 + min) + hour \right) \quad (1)$$

$$JD\ 2000 = jd - 2451545$$

4 ORBIT PROPAGATOR BLOCK

The J2 propagator is developed as an orbit propagator that only includes the perturbations due to the earth oblateness effect. Although the SGP4 or the HPOP propagator will model the spacecraft in its nearly true orbit, but will drastically slow down the simulator. Much more effort will be put in and will not yield substantial difference at this preliminary stage. The J2 perturbation effects the right ascension of ascending node and perigee only. The true anomaly, v in the six Keplerian elements $[a, e, i, \omega, \Omega, v]$ is updated with time. For the case of circular orbits the Mean anomaly is equal to the true anomaly. The position \mathbf{r} and velocity \mathbf{v} are found using the Keplerian elements in the perifocal frame, using equation 2. The position and velocity in the ECI frame are then found using transformation matrix, as given in equation 3. The propagator block in the space environment module outputs the position and velocity in the ECF frame. This is due to the fact that the real GPS sensor determines the position and velocity of the spacecraft in the ECF frame. Thus one other transformation from the ECI to ECF frame is done to finally obtain the position and velocity in the ECF frame. The modeling equations in Perifocal coordinate system, as discussed in [2] and [7] are

$$\mathbf{r}_{pf} = \begin{bmatrix} r_{x-pf} \\ r_{y-pf} \\ r_{z-pf} \end{bmatrix} = \begin{bmatrix} a(1-e^2)\cos(v) \\ \frac{1+e\cos(v)}{a(1-e^2)}\sin(v) \\ \frac{1+e\cos(v)}{0} \end{bmatrix}$$

$$\mathbf{v}_{pf} = \begin{bmatrix} v_{x-pf} \\ v_{y-pf} \\ v_{z-pf} \end{bmatrix} = \begin{bmatrix} -\sin(v)\sqrt{\frac{\mu}{a(1-e^2)}} \\ (e+\cos(v))\sqrt{\frac{\mu}{a(1-e^2)}} \\ 0 \end{bmatrix} \quad (2)$$

The position and velocity in ECF frame are then obtained, as discussed in [1], as follows

$$\mathbf{r}_e = T_{ei} \cdot T_{pi} \cdot \mathbf{r}_{pf}$$

$$\mathbf{v}_i = \dot{T}_{ei} \cdot T_{pi} \cdot \mathbf{r}_{pf} + T_{ei} \cdot T_{pi} \cdot \mathbf{v}_{pf} \quad (3)$$

4.1 Coordinate Transformations

The two coordinate transformations used in the space environment module are the

1. Perifocal to ECI Transformation, and
2. ECI to ECF Transformation

The perifocal to ECI coordinate transformation [2] is

$$T_{pi} = \begin{bmatrix} \cos\Omega\cos\omega - \sin\Omega\sin\omega\cos i & -\cos\Omega\sin\omega - \sin\Omega\cos\omega\cos i & \sin\Omega\sin i \\ \sin\Omega\cos\omega + \cos\Omega\sin\omega\cos i & -\sin\Omega\sin\omega + \cos\Omega\cos\omega\cos i & -\cos\Omega\sin i \\ \sin\omega\sin i & \cos\omega\sin i & \cos i \end{bmatrix}$$

where i is the inclination, ω is the argument of perigee, and Ω is the right ascension of the ascending node.

The second coordinate transformation could be found by combining the earth rotation angle information with the Earth nutation and precession matrix, found in [1], as

$$T_{ei} = \theta \cdot N \cdot P \quad (4)$$

where $N \cdot P$ is the product of Earth nutation and precession matrix. The earth rotation matrix θ is derived using the angle between the vernal equinox and the Greenwich meridian which is related to Greenwich Mean Sidereal time (θ_{GMST})

$$\theta_{GMST} = \theta_{GMST,2000} + \omega_e t \quad (5)$$

where $\theta_{GMST,2000}$ is value at 00:00:00 on 1st January, 2000 and is the JD2000 in seconds, and $\omega_e = 7.2921 \times 10^{-5}$ rad/s is the Earth's angular velocity.

$$T_{ei} = \begin{bmatrix} \cos(\theta_{GMST}) & \sin(\theta_{GMST}) & 0 \\ -\sin(\theta_{GMST}) & \cos(\theta_{GMST}) & 0 \\ 0 & 0 & 1 \end{bmatrix}$$

The nutation and precession matrices are not computed onboard but they could be uploaded regularly via

Telecommand in real satellites. Thus, the transformation is accurate enough without including the nutation and precession effects. The position vector and velocity in ECF are calculated as

$$\begin{aligned} r_e &= T_{ei} r_i \\ v_e &= T_{ei} v_i + \dot{T}_{ei} r_i \end{aligned} \quad (6)$$

4.2 GPS Time

The GPS time is the time provided by the GPS sensor updated using atomic clocks from the GPS constellation. This time corrects the OBC time generated by the onboard crystal oscillator. The GPS time starts from 06th January, 1980. It has an offset of 7300.5 days from the JD2000. The offset is added to the JD2000 time along with the addition of 13 seconds. The 13 second is the error in the UTC time currently in the year 2010.

4.3 Earth's Magnetic Field Model

In order to tests the attitude algorithms that are based on magnetometer measurements, for example the detumbling mode, magnetic model is required. The accuracy of the model will in turn affect the accuracy of the controlling gains. The standard model used to model the magnetic field of the Earth is World Magnetic Model (WMM). The altitude of the spacecraft is determined using ECF to LLA (Latitude, Longitude and Altitude) block, available in MATLAB version 2008. The WMM block receives the altitude, latitude and longitude of the spacecraft and computes the corresponding magnetic field of the Earth.

4.4 Sun Position And Eclipse Flag Generator

This block models the position of the sun as well as the flag is generated indicating the start and stop of the solar eclipse. The sun position is modeled according to [4] and [5]. The model takes the Julian date as input and gives position of sun in ECI frame. The eclipse is based on conical shadow model according to [2] and [5]. The eclipse flag models the full sunlight, partial eclipse and the full eclipse. The flag generates zero for full sunlight, 0.5 for penumbra (partial eclipse) and 1 for umbra (full eclipse).

4.5 Spacecraft Attitude Kinematics And Dynamics

The spacecraft attitude can be represented in variety of ways. Quaternions are most commonly used in describing the attitude, while developing attitude control algorithms. The quaternion representation has an advantage that it has a convenient product rule for successive rotations. It avoids the singularity encountered in the Euler angle representation. The attitude kinematics determines the angles and the dynamics determines the rates. The attitude kinematics modeled in quaternion representation, as discussed in [1], [3] and [7] is

$$\begin{bmatrix} \dot{q}_1 \\ \dot{q}_2 \\ \dot{q}_3 \\ \dot{q}_4 \end{bmatrix} = \frac{1}{2} \begin{bmatrix} 0 & \omega_z & -\omega_y & \omega_x \\ -\omega_z & 0 & \omega_x & \omega_y \\ \omega_y & -\omega_x & 0 & \omega_z \\ -\omega_x & -\omega_y & -\omega_z & 0 \end{bmatrix} \begin{bmatrix} q_1 \\ q_2 \\ q_3 \\ q_4 \end{bmatrix} \quad (7)$$

where ω_x , ω_y , and ω_z are the angular velocities in the x, y and z-axes respectively.

The spacecraft dynamics is driven by the external torques applied. The dynamics equation, according to [1], is as follows

$$T = T_{dist} + T_{mgt} = I\dot{\omega} + \omega \times (I\omega + h_{RW}) + \dot{h}_{RW} \quad (8)$$

where T is the external torque, that is the sum of T_{dist} and T_{mgt} . First term is the disturbance torque and the latter is the magnetic torquer's torque. \dot{h}_{RW} is the torque exerted by the Reaction Wheel on satellite. The direction of the Reaction Wheel Torque will be opposite to the satellite rotation. I is the time invariant Inertia matrix. ω is the angular rate of satellite. h_{RW} is the angular momentum of the reaction wheels.

5 DISTURBANCES BLOCK

The significant disturbances in Low Earth Orbits (LEO) are the Gravity-Gradient Disturbances, Solar Radiations, Earth's Magnetic Field and the Aerodynamic Forces, according to [6]. The Solar Radiations and the Aerodynamic Forces effects the geometric center where this force results in torque around the center of mass. The other two disturbances directly acts the torque on the spacecraft. The disturbances are model as constant values that keep on acting as the simulation goes on. The Gravity gradient disturbance acts due to uneven gravitational pull. Although it is required for spin stabilized satellites, but most of the low earth orbit satellites are three axis stabilized. Torques generated by the effects of solar pressure is, unlike the other disturbances, generally independent of orbital altitude. In LEO, this disturbance is insignificant. The third disturbance is generated by interaction between the spacecraft residual magnetic dipole and the Earth's magnetic field. The Aerodynamic drag is the most significant force in LEO which originates from the coalition between gas molecules in the atmosphere and the satellite. The total disturbance is the sum of all the above secular disturbances and is added with the magnetic torque MTQ torque to sum up the total external forces acting on the satellite. These external forces added with the Reaction Wheels Torque (opposite in the direction of satellite rotation) to form the Torque input of Spacecraft Attitude Kinematics and Dynamics block, as shown in the Figure 4.

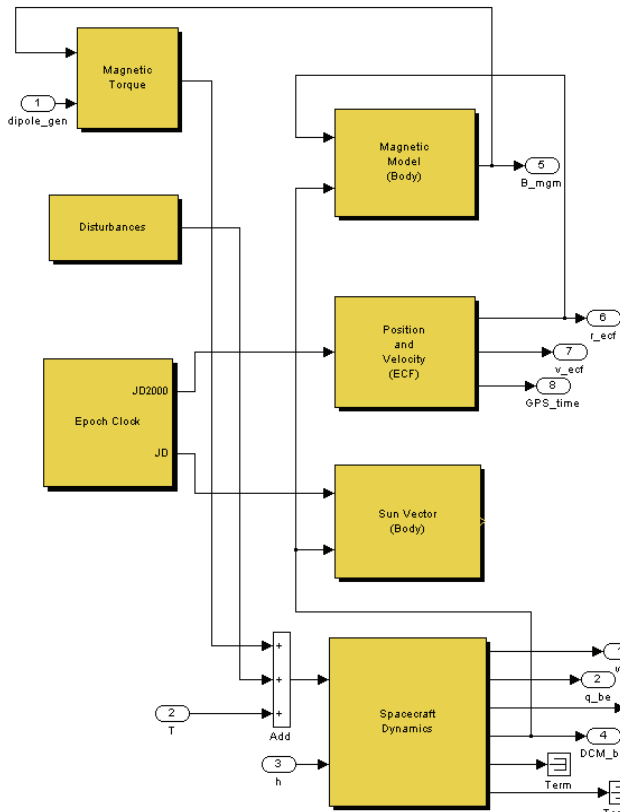


Figure 4 - Space Environment Module Layout

6 SIMULATION VERIFICATION

The Space Environment block was verified by comparing the results of MATLAB/Simulink with the STK. For the said purpose, actual parameters of low-earth orbiting Korean satellite, KOMPSAT has been used, according to [7] and [8]. The Korea Multi-Purpose Satellite-1 (KOMPSAT-1) was successfully launched by the Taurus launch vehicle at 07:13:00 UT, December 21, 1999, from Vandenberg Air force Base, California, U.S.A. The KOMPSAT is a sun-synchronous remote sensing satellite with the inclination of 98.13 degrees, the altitude of 685 km, and the total weight of 509 kg. The orbital period is 98.5 minutes, that is, around 5910 seconds. The start time for the simulation is set to 1st July, 12:00:00.00 UTCG, 2006. The Keplerian elements of Kompsat-1 are $[a, e, i, \omega, \Omega, \nu] = [7063.269, 0.00561, 98.1265, 0, 0, 360]$ [7].

The simulations are performed for position and velocity in ECF Frame, Sun Position and Magnetic Field in ECI Frame, both in STK and the Space Environment Module (MATLAB/Simulink) represented in Figures 5-8. The difference in the STK simulations and MATLAB results increases with time. The models are accurate enough to sustain the difference to a very much low value for 2 to 3 orbits, as represented in Figure 9 and 10. Thus providing enough time to verify the attitude and orbit control algorithms. These verified algorithms will then act as a platform for the

real time testing and will certainly reduce the development time of fully verified AOCS algorithms.

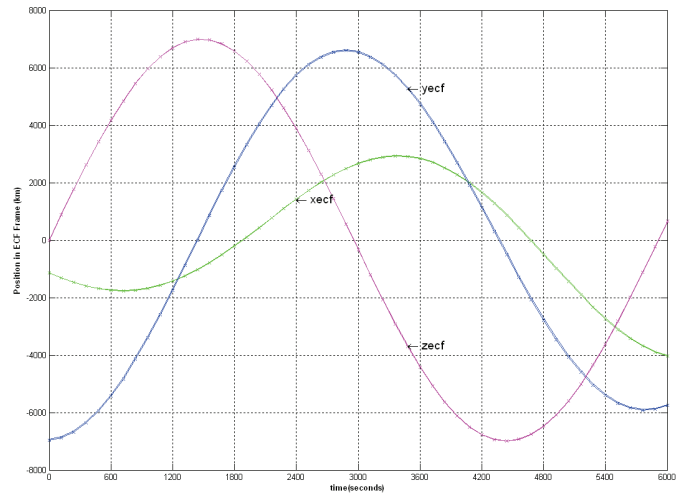


Figure 5 - ECF position of KOMPSAT-1, STK results are in 'x' overriding the MATLAB results

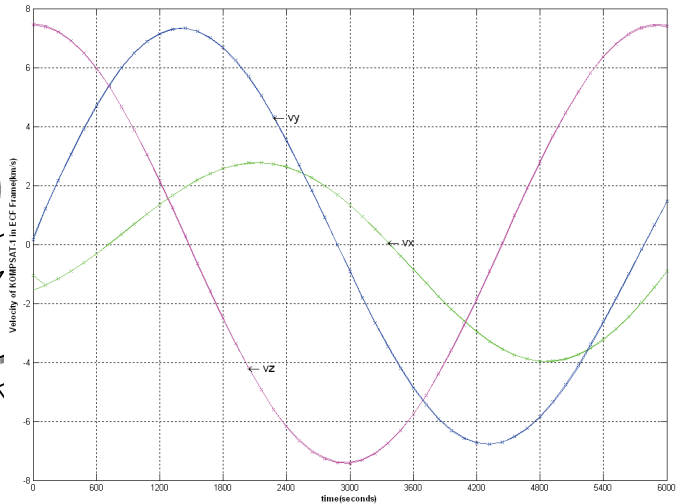


Figure 6 - ECF velocity of KOMPSAT-1

The Kompsat-1 Inertia matrix, as given in [9], is

$$I = \begin{bmatrix} 29462 & 0 & 0 \\ 0 & 12956 & 0 \\ 0 & 0 & 20976 \end{bmatrix} \quad (9)$$

The attitude algorithms for AOCS subsystem are designed for various modes, depending upon the mission requirements. The magnetometer and magnetotorquers are used for the detumbling mode. The angular velocities at the time of satellite separation from the launcher are assumed to be $[3, -2, 1]$ deg/s. The Torque rods are assumed to provide 50 Am^2 Dipole. The results for the detumbling mode for verification of spacecraft attitude kinematics and dynamics block are given in Figure 11 and 12. The detumbling mode could not be modeled in STK. Thus, the detumbling of the angular velocities in approximately 2 orbits is quite enough verification for the

block. The detail modeling of the detumbling mode is beyond the scope of this paper.

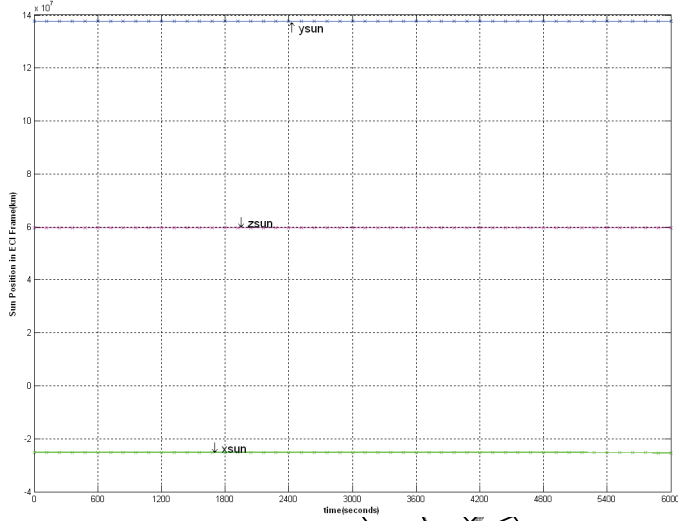


Figure 7 - Sun Position of KOMPSAT-1

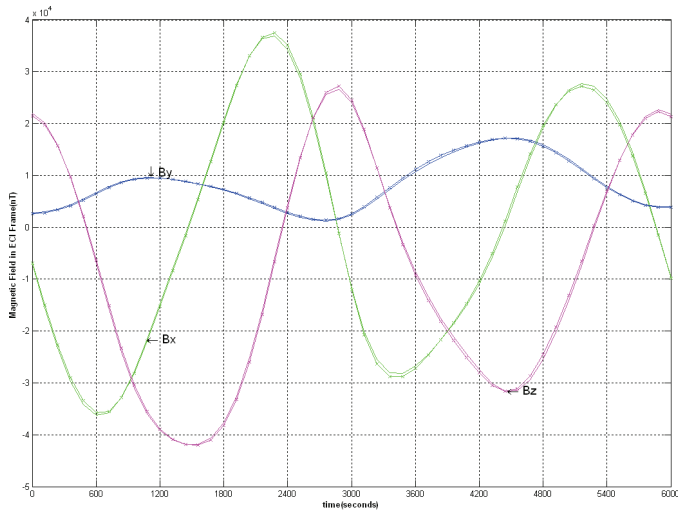


Figure 8 - Magnetic Field of KOMPSAT-1

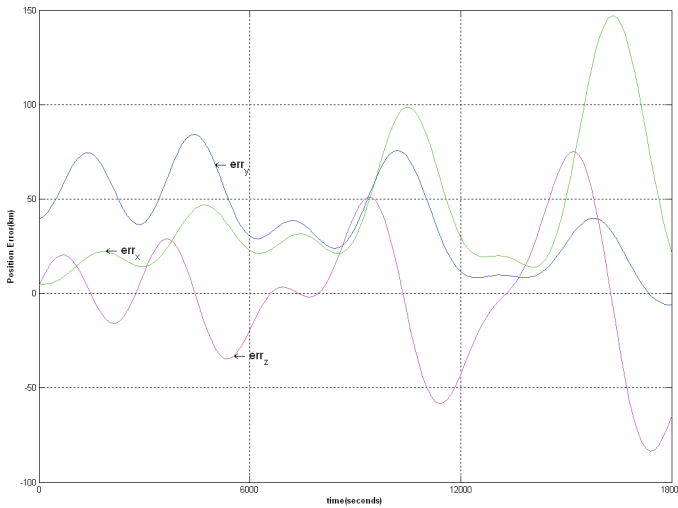


Figure 9 - Position Error in STK and MATLAB results

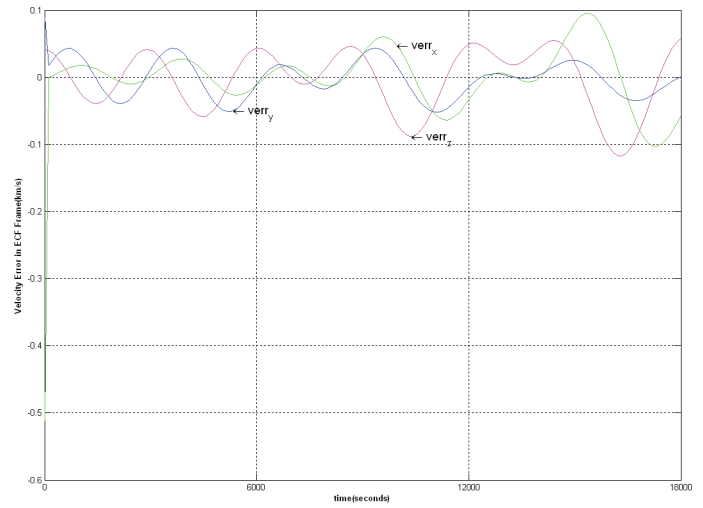


Figure 10 - Velocity Error in STK and MATLAB results

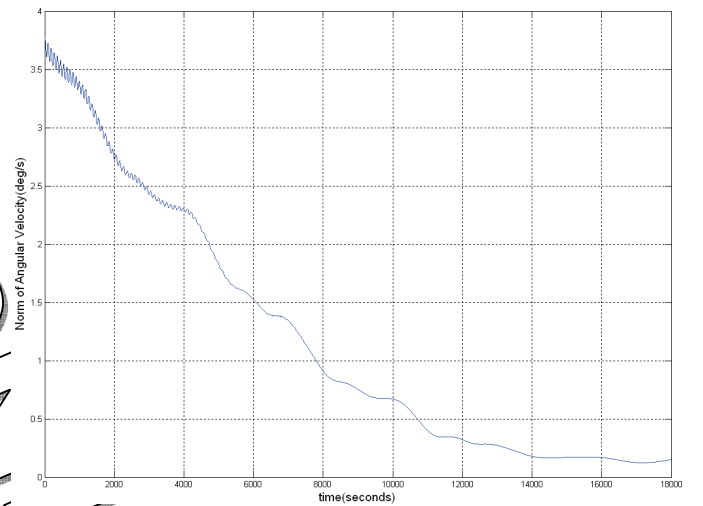


Figure 11 Detumbling of angular velocity norm

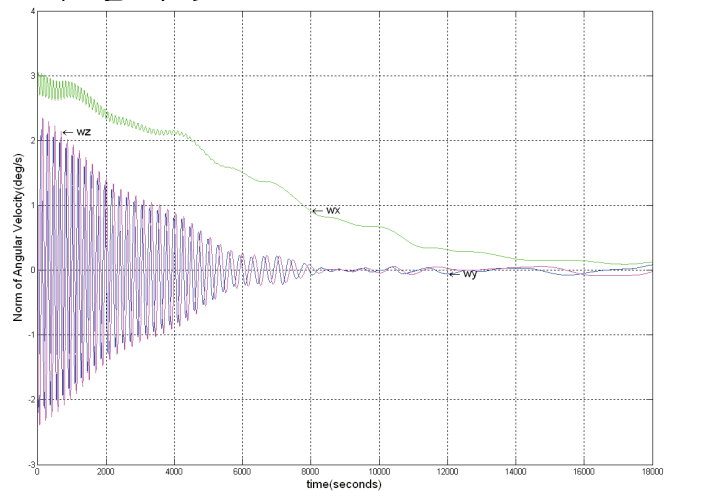


Figure 12 Angular Velocities along the three axes detumbling to zero

7 CONCLUSION

The development of Space Environment Module for LEO satellites is introduced in this paper. The module is a part of a bigger exercise, that is, the development of a complete AOCS Simulator. Every time the satellite project starts, only the mission parameters are to be entered and the attitude algorithms will be developed based on the selected sensors and actuators in the AOCS Simulator. The module mainly contains the epoch clock, orbit propagator block, disturbances, magnetic field model, sun model and spacecraft attitude kinematics and dynamics block.

The space industry mainly uses the space environment module for verifying its attitude control algorithms before validating it on three-axis air-bearing table. For small satellites it is being explored to directly embed the attitude control algorithms to use it on the satellite without any requirement of testing on air-bearing test bed. The space environment module drastically cuts down the time in developing the AOCS subsystem for satellites in low earth orbits.

ACKNOWLEDGEMENTS

We would like to thank SUPARCO people for helping us throughout the project, specifically; we want to mention Dr. Muhammad Yasir for his guidance and support. We also wish to acknowledge Mr. Fahad Tanveer for his valuable advices, and finally to all the members of AOCS Section, SRDC, Karachi for their support in the design of individual subsystems of the module.

REFERENCES

- [1] Muhammad Yasir, *Development and Implementation of attitude control algorithms for the micro-satellite Flying Laptop*, Ph.D Thesis, Institute for Space Systems, Universität Stuttgart, 2010.
- [2] James R. Wertz, *Mission Geometry; Orbit and Constellation Design and Management*, Microcosm Press, EI Segundo, California, 2001.
- [3] James R. Wertz, *Spacecraft Attitude Determination and Control*, D. Reidel Publishing Company, Dordrecht, Holland, 1978.
- [4] David Vallado, *Fundamentals of Astrodynamics and Applications*, 2007.
- [5] Oliver Montenbruck, Gill Eberhard, *Satellite Orbits: Models, Methods and Applications*, Springer Verlag, 2000.
- [6] Rouzbeh Amini, Jesper A. Larsen, Roozbeh Izadi-Zamanabadi, Dan D. V. Bhandari, *Design and Implementation of a Space Environment Simulation Toolbox for Small Satellites*, 56th International Astronautical Congress 2005.
- [7] Hyo-Sung Ahn and Seon-Ho Lee, *Gyroless Attitude Estimation of the Sun-Pointing Mode Satellite*, ICCAS2003.
- [8] <http://earth.esa.int/object/index.cfm>.
- [9] Chang-Hee Won, *Comparative study of various control methods for attitude control of LEO satellite*, Aerospace Science and Technology, 1999.